MOISTURE- AND FREEZE-THAW-INDUCED DETERIORATION OF NATURAL FIBER COMPOSITES WITH LOW FIBER CONTENTS

K. Noonan[1], K. Hess[1], W. Srubar[1]

[1]Department of Civil, Environmental, and Architectural Engineering, University of Colorado Boulder, ECOT 441 UCB 428, Boulder, Colorado, USA

*Corresponding author; e-mail: wsrubar@colorado.edu

Abstract

Social, political, and environmental pressures continue to drive the development of sustainable alternatives to petroleum-based materials. Accordingly, natural fiber composites (NFCs) are being developed and used for a range of low- and high- performance applications, such as packaging, automotive parts, and construction materials. As the use of NFCs become more widespread, there is a rising need to investigate the effect of weathering on this emerging class of materials. Previous studies on the moisture and freeze-thaw induced deterioration of NFCs have focused primarily on composites with high fiber contents (>50% by volume). Due to factors, such as low cost, bio-renewability, and enhanced mechanical properties, most commercially available NFCs maximize the content of natural fibers. However, high fiber contents also increase susceptibility to the deleterious effects of environmental aggressors (e.g., moisture and temperature).

Since limited data exists on the durability of low-fiber content NFCs, this study investigates the moisture-induced deterioration of NFCs with low fiber content and explicitly analyzes the added effects due to freezing and thawing. Results from a combination of environmental conditioning and X-ray tomography provide and visual evidence of the effect of moisture-induced damage in low-fiber NFCs. Results also show that this deterioration is exacerbated by below-freezing temperatures. Investigating the response of NFCs to such environmental aggressors as demonstrated in this study provides an evidenced-based approach for material design, which ultimately depends on both the intended application and expected environmental conditions.

Keywords:

Natural-fiber composites; moisture-induced deterioration; freeze-thaw durability; mechanics; x-ray tomography

1 INTRODUCTION

The future market for natural fiber composites (NFCs) is expected to grow due to continued social and political pressures for sustainable alternatives to petroleum-based materials [Väisänen 2016]. Conventionally, fiber reinforced composites (FRPs) have been fabricated with synthetic petroleum-based fiber reinforcement (e.g., carbon, glass, and aramid) and synthetic polymer matrices (e.g., polypropylene, polyethylene, and epoxy) [Netravali 2003, Netravali 2014, La Mantia 2011]. In an effort to minimize reliance on fossil fuels and reduce environmental impacts, lignocellulosic natural fibers (e.g., wood, flax, ramie, hemp, jute, abaca, kenaf, and sisal) have been incorporated as fiber reinforcement within synthetic and biobased polymer matrices. In particular, hemp species are emerging as a more commonly selected natural fiber reinforcement due to good mechanical properties, renewability, and increased availability as a result of government legislation [Dhakal 2007, Holbery 2006].

Fully biobased NFCs have natural fiber reinforcement within a biobased polymer matrix (e.g., polylactic acid, polyhydroxybutyrate, and bio-derived polyethylene) [Netravali 2003, Netravali 2014, La Mantia 2011, Srubar 2012]. This emerging class of fully biobased NFCs aims to reduce environmental impacts by shifting from petroleum-based to fully bio-renewable resources. When placed in landfills, the inherent biodegradable compositions of fully biobased NFCs contribute to minimizing degradation time. In addition, during the degradation process, products (e.g., methane, water, and carbon dioxide) are released, which can be repurposed for biofuel or the manufacture new NFCs, thus achieving a closed-loop lifecycle [Mohanty 2005, Srubar 2012, Srubar 2011, Ryan 2017].

Although natural fibers are a low-cost bio-renewable filler with high mechanical properties, their chemistries contain molecular groups that have an affinity for water molecules. Absorbed moisture negatively affects the bonding of the chemical constituents and reduces the mechanical properties of the fiber [Niska 2008]. In addition, the associated fiber particle volume increases with moisture absorption (due to swelling), which results in matrix cracking and subsequent loss of composite mechanical properties [Srubar 2013]. This deterioration mechanism is exacerbated in freezing conditions when the absorbed water freezes and expands [Srubar 2015]. Therefore, freeze-thaw deterioration is a common cause for repair and replacement of construction materials [Pilarski 2005]. Previous studies have

investigated the response of NFCs undergoing freeze thaw cycles and the decreased surface bond between fiber and polymer matrix. Studies have found that as the fibers experience saturation and an additional expansion due to freezing temperature the matrix structure is compromised and loses mechanical properties associated with the strength of the polymer matrix [Adhikary 2008, Wang 2007]. Previous studies have primarily investigated NFCs with high fiber contents (>50%) [Pilarski 2005, Pilarski 2006, Wang 2007]. Reducing the fiber content of NFCs may improve resistance to the deleterious effects of environmental aggressors compared to high-fiber content NFCs, but the durability data on low-fiber composites remains limited.

In this study, hemp and green polyethylene composites with low fiber volume fraction, namely 15%, and 30%, were exposed to moisture and freeze-thaw conditions. Moisture sorption isotherms for composite disk samples were experimentally obtained and computationally predicted using Fick's laws of moisture diffusion. Composite samples were immersed in deionized water at three temperatures (i.e., 4°C, 22°C, and 39°C) in order to determine the effect of temperature on the rate of moisture diffusion. One 15% fiber volume fraction sample and one 30% fiber volume fraction sample were placed in freezing conditions after fully saturated with moisture at 39°C. Micro-computerized tomography was used to compare the void content unconditioned, fully saturated, and frozen composite samples of 15% and 30% fiber volume fraction. This study aims to investigate the effect of moisture-induced compared to freeze-thaw-induced deterioration on hemp composites with low fiber volume fraction.

2 EXPERIMENTAL PROGRAM

2.1 Materials

The materials used to complete this study include green polyethylene and hemp fiber pellets at 30% fiber volume fraction (GPE HC200500, Green Dot Bioplastics, Kansas) and neat green polyethylene pellets (GPE HC200500, Green Dot Bioplastics, Kansas), and deionized (DI) water.

2.2 Composite Fabrication

Composite Processing

Composite samples were prepared by combining neat green polyethylene pellets and the hemp fiber pellets in order to create varying fiber content for the experimental samples. The composite formulations used in this study are provided in **Table 1**. Prior to composite extrusion and injection molding the samples, the polymer and composite pellets were dried at 50°C for a duration of 24 hours. After drying, the pellets were massed and separated to produce the composite formulations for testing (**Table 1**). Experimental disc samples containing 15% fiber volume required 3.5 grams of neat green polyethylene pellets and 3.5 grams of 30% fiber content pellets. Experimental disc samples containing 30% fiber volume required 7.0 grams of 30% fiber content pellets.

Tab.10: Sample nomenclature and compositions of fabricated composites for experimental testing

Sample Nomenclature	Fiber Volume Fraction	Polymer	Fiber
GPE+H0	0 %	Green Polyethylene	Hemp
GPE+H15	15 %	Green Polyethylene	Hemp
GPE+H30	30 %	Green Polyethylene	Hemp

Composite Processing

After the appropriate masses were determined, the proportioned pellets were placed in a micro compounder with conical twin-screws (HAAKE Minilab II, Thermo Scientific, Waltham, MA). The process for 15% fiber volume fraction composite samples required alternating the neat polymer pellets and the fiber containing polymer pellets in order to create homogeneity within the samples. The compounder mixed the sample material at a screw speed of 140 rpm for a 3 minute duration. At the end of the mixing cycle, the sample mixture was extruded into the injection gun of the injection molding system (HAAKE MiniJet Pro Piston Injection Molding System, Thermo Scientific, Waltham, MA).

2.3 Experimental Methods

Isothermal Sorption

The manufactured composites were exposed to immersion conditions at three distinct temperatures (i.e., 4°C, 22°C, 39°C). Composite samples listed in **Table 1** were tested in triplicate. Prior to testing, immersion temperature conditions were ensured by pre-conditioning the deionized water to the desired temperatures (i.e., 4°C, 22°C, 39°C) for 48 hours. The temperature of the deionized water was monitored using temperature and humidity commercial recording devices (EL-USB-2-LCD, Lascar Electronics, Erie, PA). In addition, to confirm the temperature data accuracy, periodic direct temperature measurements were performed with a standard lab-grade mercury thermometer. After immersion chambers attained desired conditioning temperatures, the diameter and thickness of each composite sample was determined via caliper measurements and the mass of the sample was recorded using a balance (XS105, Mettler Toledo, Columbus, OH). Samples were then immersed at each temperature condition and covered with mesh to keep fully submerged. In order to determine the moisture content, the samples were massed at increasing time increments according to a modified ASTM D570 procedure. The moisture content (M_t) at each time interval was determined as weight percent of total sample weight, using the following equation:

$$M_t = \frac{m_t - m_0}{m_0} \, x \, 100\% \quad (1)$$

where m_t is the mass of the sample at a given time interval and m_0 is the initial mass of the sample after preconditioning.

Throughout the duration of the sorption, periodic measurements were recorded to determine dimensional changes. The values of the % volume change can be found in **Table 3**. The % dimension change was calculated by:

$$\% \Delta = \frac{Measured\ Dimension - Initial\ Dimension}{Initial\ Dimension} \quad (2)$$

Freeze-Thaw Degradation

After saturation, two composite samples with 15% and 30% fiber volume content, respectively, were exposed to one freeze thaw cycle. Post immersion, the samples were placed in freezing conditions for a 72 hour duration. After the 72 hour duration samples were moved into a temperature controlled oven at 40°C for an additional 72 hours to remove any moisture present in samples. Mass and dimension measurements were completed and recorded both before and after placement in each new environmental condition.

Micro-Computerized Tomography

The quantification of void space present within composites was completed through a non-destructive imaging process. Composites were analyzed using micro-computerized tomography (Xradia Versa XRM-520, Zeiss, Dublin, CA) to construct a three-dimensional image. The three-dimensional image was completed over a 16 hour scan duration with 30 second frame exposure time, a 4x magnification factor, air filter, and specific energy settings of 40.0 kV and 3.0 W.

Post processing of the image was completed through a segmentation software (Dragonfly 3.6 (Object Research Systems (ORS) Inc, Montreal, QC). The segmentation process allowed the varying constituents of the composite to be accurately identified and quantified in order to analyze the matrix and fiber structural changes that occur through various condition processes (i.e., moisture saturation, freeze-thaw cycle). This was completed through the segmentation of a representative cube of a cropped portion of the three-dimension scan of the composite. The representative cube can be analyzed to obtain volumetric quantities of the various constituents. Samples which experienced saturation at 39°C and saturation and a freeze-thaw cycle were analyzed through micro-computerized tomography and compared to an unconditioned sample.

3 THEORETICAL FORMULATION

3.1 Fick's Laws and Diffusion Coefficient

The governing moisture diffusion behavior in materials, such as Fickian or anomalous, is commonly determined using the following power law equation proposed by Alfrey (1966):

$$\frac{M_t}{M_\infty} = kt^n \quad (3)$$

where M_t is the moisture content at time (t), M_∞ is the equilibrium moisture content, k is a kinetic constant characteristic of the polymer network, and n is a constant that classifies the diffusion behavior. For polymeric materials, $n = 0.5$ indicates Fickian diffusion, $0.5 > n > 1$ indicates anomalous transport, and $n = 1$ indicates relaxation-controlled transport.

For Fickian diffusion behavior, the diffusion coefficient (D) refers to the rate at which solvent molecules (e.g., water) permeate a solute (e.g.,) the composite and is determined as follows:

$$D = D_A\left[1 + \frac{h}{r}\right]^{-2} \quad (4)$$

where h is the thickness of the sample (mm), r is the radius of the sample (mm), the edge correction factor (ECF) for disk samples is defined as the positive square of the quantity in brackets, and D_A is the apparent diffusion coefficient which is calculated according to:

$$D_A = \frac{\pi h^2 \theta^2}{16 M_\infty{}^2} \quad (5)$$

Where θ is the initial slope of the experimental sorption curve $(\%/\sqrt{hr})$. In order to apply the theoretical Fickian diffusion model, the following assumptions are considered. First, the material is homogeneous. Second, moisture diffusion transpires such that all moisture is transferred through the planar faces not through the edges. Third, the boundary conditions remain constant. Lastly, the material has a constant moisture concentration profile before exposure to moisture. Therefore the moisture transport through a plane sheet can be described by [Srubar 2012]:

$$\frac{M_t}{M_\infty} = 1 - \frac{8}{\pi^2}\sum_{n=1}^{\infty}\frac{2}{(2n-1)} exp\left[\frac{-D(2n-1)^2\pi^2 t}{h^2}\right] \quad (6)$$

where M_∞ is determined according to [Srubar 2012]:

$$M_\infty = w_f[0.3 - 0.001(T - 20)] \quad (7)$$

where w_f is the percent weight fraction of fiber and T is the temperature (K).

Due to the triplicate testing all calculation values provided an average and standard deviation, which were utilized to implement a Monte Carlo simulation within the predictive model to create an accurate range of anticipated values based on the error associated with experimental data collected. The simulation is set to run 10,000 iterations in order to create a standard error related to the specific properties and diffusion coefficients calculated from experimentation.

4 RESULTS AND DISCUSSION

4.1 Isothermal Water Sorption

The collected experimental moisture sorption data is shown in **Figure 1**. These moisture curves are utilized to determine the diffusion properties of the various composites. The composites conditioned at the lowest temperature of 4°C exhibited the slowest rate of moisture sorption. The highest moisture content that the composites reached was 3.5% by weight. This equilibrium moisture content is seen in the samples containing 30% fiber by volume. Comparatively the composite samples with 15% fiber by volume reaches a lower equilibrium moisture absorption of just above 1%.

The difference between the highest recorded moisture content values is expected. Samples that contain a higher amount of fiber have a higher moisture potential within the sample. The wood fibers exhibit hydrophilic properties and due to the increase of the amount of fiber in the 30% fiber volume samples they attain the ability to absorb more moisture within the entire volume of the sample.

The samples conditioned at 22°C display an increased absorption rate when compared to 4°C conditioned samples. The largest recorded moisture content for the 22°C samples was found to be 9% for composites consisting of 30% fiber content by volume and 3% for composites containing 15% fiber content by volume. Again, the increase in moisture absorption between the composite formulations is expected due to the increase in the fiber content within the composites. The increase in moisture content between the two distinct temperature conditions is also expected. As the temperature of the conditioning chambers increase the water molecules are more rapidly moving through the medium. The increased speed of the water molecules

allows for a faster transport into the composite sample and therefore an increase in moisture potential for the fibers to absorb a larger quantity of moisture at a faster rate.

The same trends are present when analyzing the highest temperature conditioned composites. These samples were conditioned at 39°C. The highest recorded moisture content is 10.5% for samples containing 30% fiber and just over 4% for samples containing 15% fiber. Again, there is an observed increased sorption rate at a higher temperature as indicated by the increased slope in the experimental data. The data shows an increase when comparing 30% fiber volume samples, however the increase is not as drastic with the samples containing 15% fiber. This is expected as there is more fiber there is most likely fiber closer to the surface area of the sample making the moisture transport distance shorter and therefore allows the sample to absorb a larger amount of moisture over the same time period.

As expected, the increase in moisture content within the composites resulted in a dimensional change in addition to a mass change.

The results prove that due to the additional uptake of water the disc samples experience an increase in the overall height of the samples. For samples exposed to higher temperatures, the volume change recorded is greater. This is anticipated based on the amount of moisture these samples have retained in comparison to the samples conditioned at lower temperatures. Similarly, the same trend is identified between samples of 30% fiber content and 15% fiber content. Composites with higher fiber content have a larger dimensional increase.

Additionally, the samples do not show expansion in the radial direction. This may be due to the orientation of the fibers within the composite. The fibers will have greater expansion in the transverse direction and most likely the orientation of the fibers is such that the transverse expansion corresponds to a dimensional change in height of the samples.

Tab. 2: Composite dimension changes post saturation

		Fiber Volume Fraction		
		0 %	**15%**	**30%**
4° C	**D (mm.)**	0.0%	-0.1%	-0.3%
	H (mm.)	-0.1%	0.6%	1.7%
22° C	**D (mm.)**	0.0%	0.3%	0.5%
	H (mm.)	0.0%	4.4%	7.3%
39° C	**D (mm.)**	0.0%	-0.2%	0.4%
	H (mm.)	0.1%	4.2%	11.1%

4.2 Predictive Diffusion Modeling

A computational model was developed from Fick's law of diffusion described in Section 3.0. As shown in **Figure 2,** the model can accurately predict the diffusion of various fiber content samples as well as predict at a variation of temperatures. **Table 4** lists the calculated diffusion coefficients for the various composites as well as the predicted equilibrium moisture content, M_∞. In all three temperature conditions, the model includes error which was incorporated into the model through the implementation of a Monte Carlo Simulation.

The predicted equilibrium moisture content does not vary greatly between temperature conditions, however, the expected time it will take samples to reach equilibrium decreases as the temperature value increases. The calculated value for the equilibrium moisture content is most sensitive to the fiber volume content, which causes the difference in the equilibrium moisture content values between samples contain 15% fiber versus 30% fiber. Samples with 30% fiber content are predicted to reach values of 8.43% while samples with 15% fiber content are anticipated to reach 4.22%.

The time to reach equilibrium varies between the temperature conditions. A higher temperature results in a decreased time to reach the predicted equilibrium content, while lower temperatures cause and extended duration in order to reach the predicted equilibrium value. **Figure 2** displays this relationship between temperature condition and time to equilibrium.

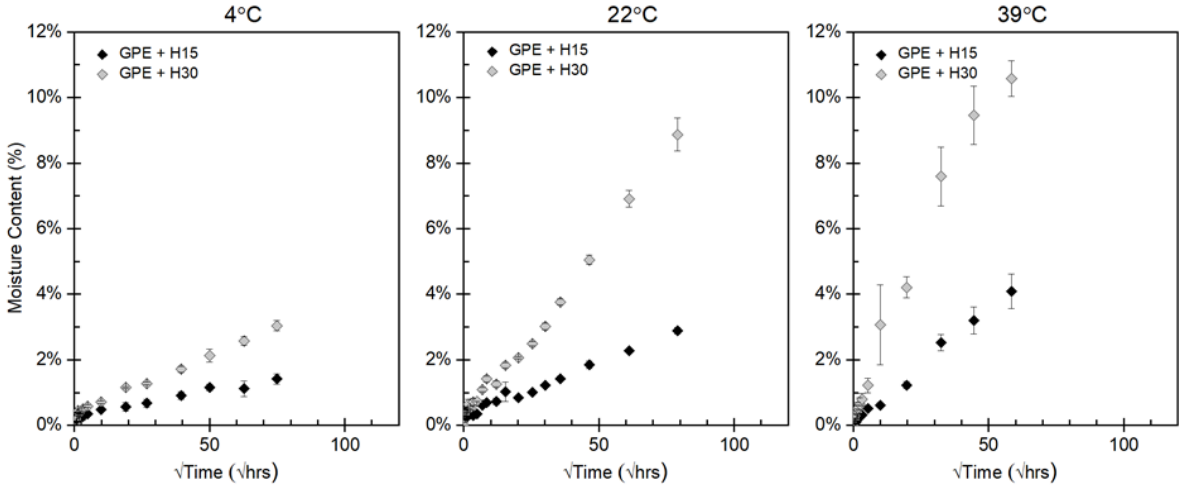

Fig 79: Experimental isothermal moisture sorption curves

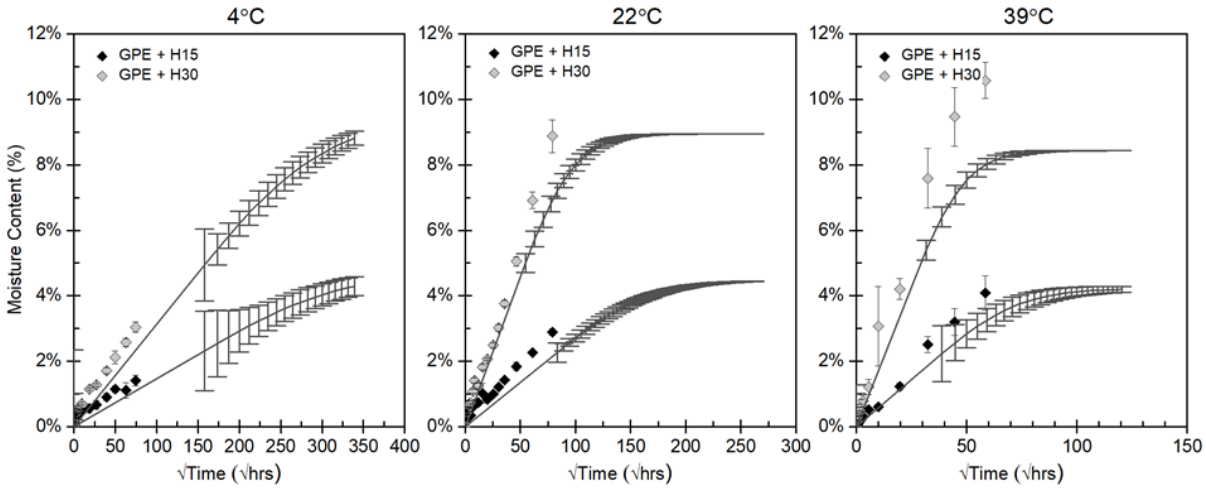

Fig. 80: Predictive Fickian diffusion model derived with experimental diffusion coefficients

4.3 Freeze-Thaw Degradation

Quantification of the degradation induced by a freeze-thaw cycle was conducted through comparison of micro-computerized tomography of three samples, each exposed to a different environmental condition. **Figure 3** displays the visual comparison between 2D slices of the segmented composites. Samples include a control sample (unconditioned), a saturated sample at 39°C, and a saturated sample at 39°C exposed to a freeze thaw cycle. The red portions of the images indicate the void space present within the sample.

There is an increase in the visible quantity of void between samples that have been unconditioned and samples that have been exposed to saturated conditioning. Samples that were additionally exposed to a freeze-thaw cycle experience secondary deterioration as noticed by the increase in the red void space in **Figure 3**.

The increase in void space between the unconditioned sample and the saturated sample is expected. It is understood that the absorption of moisture by a hydrophilic material such as natural fiber increases the volume of that material. The fiber gains additional moisture and swells in size. As this swelling occurs the stiff polymer matrix is experiencing tensile forces imposed by the expanding fiber and this leads to potential micro cracking within the matrix. These micro cracks are the primary reason for the increase in void space within the composite given a saturated condition.

At low fiber volume contents, the additional expansion due to freezing is expected to cause an even larger onset of deterioration. This is evident both in the two-dimensional slices in **Figure 3** as well as the **Figure 4** which displays the corresponding volume of void as a %. The largest increase in voids occurs in samples that have undergone a singular freeze-thaw cycle.

Tab. 3: Average experimental diffusion coefficients and predicted equilibrium moisture content

Temperature Condition	Fiber Volume %	Average Diffusion Coefficient (m^2/s)	Std. Dev.	M_∞
4° C	15%	4.19E-06	1.16E-06	4.73%
4° C	30%	5.87E-06	7.82E-07	9.46%
22° C	15%	2.01E-05	1.75E-06	4.47%
22° C	30%	5.24E-05	4.72E-06	8.94%
39° C	15%	1.04E-04	2.56E-05	4.22%
39° C	30%	2.00E-04	2.44E-05	8.43%

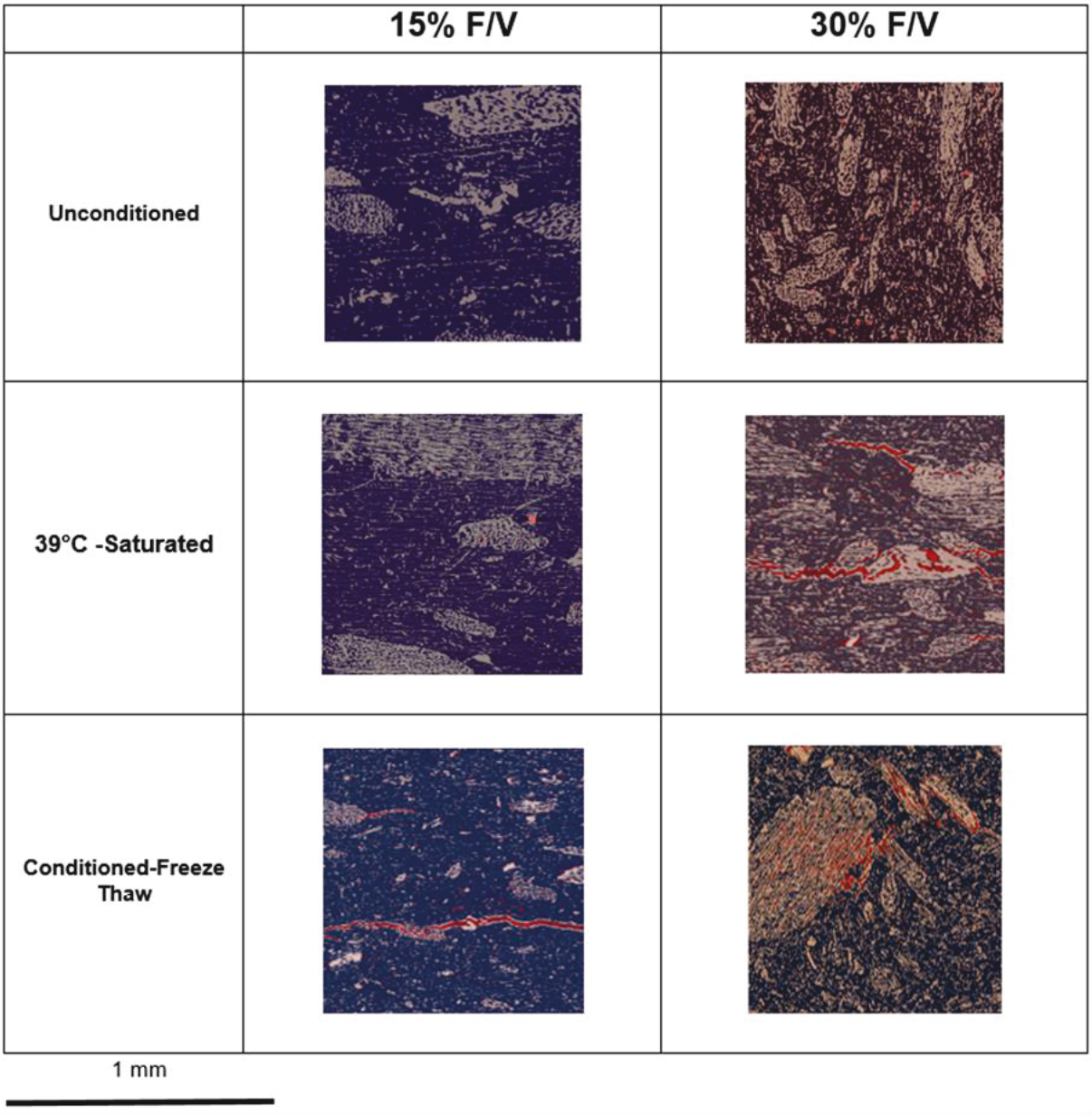

Fig. 81: Two-dimensional slices from micro-computerized tomography of various conditioned composites

5 CONCLUSIONS

Water transport in low fiber volume content natural fiber composites was investigated to determine the primary degradation that occurs due to extensive moisture exposure as well as a single freeze-thaw cycle. Water immersion was completed at three temperatures (i.e., 4°C, 22°C, 39°C) with samples of two fiber volume compositions (15% fiber content, 30% fiber content). Samples comprised with a higher content of hydrophilic hemp fiber absorbed an increased amount of moisture compared to samples with a lesser fiber content. Volumetric expansion changes were determined through incremental dimensional measurements.

Absorption curves obtained from experimental data of individual samples provided input data to produce a predictive Fickian diffusion model to determine moisture absorption of various sample compositions exposed to moisture at different temperatures.

Saturated composites subsequently exposed to a singular freeze-thaw cycle experienced additional degradation due expansion of the saturated fibers within a rigid polymer matrix structure. XRM post processing and segmentation provided quantitative analysis of the micro cracking within the matrix structure of the NFCs. The primary degradation occurs from the initial moisture absorption from immersion conditions. Similar to moisture absorption, samples with lower fiber content experience less overall structural degradation of the matrix structure when exposed to freeze-thaw cycle as the overall moisture content within the sample is not significant enough to considerable increase the micro cracking present within the structure.

To efficiently implement biological materials in building applications, degradation mechanisms which cause damage to these materials must be understdood. Natural fiber composites mechanical properties benefit from an increase in the amount of natural fiber present within the structure, but this quantity of fiber is largely associated with moisture induced deterioration. Due to

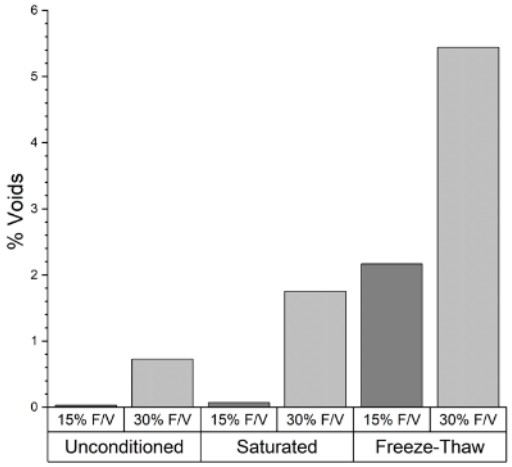

Fig 82: Quantified volume of voids from micro-computerized tomography segmentation

a large gap of information, this study aims to provide information pertaining to degradation of composites formulated from low fiber contents and the performance of composites when exposed to saturation and freeze-thaw cycles.

6 ACKNOWLEDGMENTS

This research was made possible by the Department of Civil, Environmental, and Architectural Engineering, the College of Engineering and Applied Sciences, and the Living Materials Laboratory at the University of Colorado Boulder, with support from the National Science Foundation (Award No. CMMI-1537194). Dr. Cecily Ryan and Mathew Solle in the Department of Mechanical and Industrial Engineering at the University of Montana are gratefully acknowledged for their contribution of complete composite fabrication.

7 REFERENCES

Adhikary, K. B., Pang, S., & Staiger, M. P. (2008). Dimensional stability and mechanical behaviour of wood–plastic composites based on recycled and virgin high-density polyethylene (HDPE). Composites Part B: Engineering, 39(5), 807–815. https://doi.org/10.1016/j.compositesb.2007.10.005

Alfrey T, Gurnee EF, Lloyd WG. Diffusion in glassy polymers. J Polym Sci Pol Sym 1966;12(1):249-261).

Dhakal, H. N., Zhang, Z. Y., & Richardson, M. O. W. (2007). Effect of water absorption on the mechanical properties of hemp fibre reinforced unsaturated polyester composites. Composites Science and Technology, 67(7), 1674–1683. https://doi.org/10.1016/j.compscitech.2006.06.019

Holbery, J., & Houston, D. (2006). Natural-fiber-reinforced polymer composites in automotive applications. JOM, 58(11), 80–86. https://doi.org/10.1007/s11837-006-0234-2

La Mantia, F. P., & Morreale, M. (2011). Green composites: A brief review. Composites Part A: Applied Science and Manufacturing, 42(6), 579–588. https://doi.org/10.1016/j.compositesa.2011.01.017

Mohanty, A. K., Misra, M., & Drzal, L. T. (Eds.). (2005). Natural fibers, biopolymers, and biocomposites. Boca Raton, FL: Taylor & Francis.

Netravali, A. N., & Chabba, S. (2003). Composites get greener. Materials Today, 6(4), 22–29. https://doi.org/10.1016/S1369-7021(03)00427-9

Netravali, A. N., & Pastore, C. M. (2014). Sustainable Composites: Fibers, Resins and Applications. DEStech Publications, Inc.

Niska, K. O., & Sain, M. (2008). Wood-Polymer Composites. Elsevier.

Pilarski, J. M., & Matuana, L. M. (2005). Durability of wood flour-plastic composites exposed to accelerated freeze–thaw cycling. Part I. Rigid PVC matrix. Journal of Vinyl and Additive Technology, 11(1), 1–8. https://doi.org/10.1002/vnl.20029

Pilarski, J. M., & Matuana, L. M. (2006). Durability of wood flour-plastic composites exposed to accelerated freeze–thaw cycling. II. High density polyethylene matrix. Journal of Applied Polymer Science, 100(1), 35–39. https://doi.org/10.1002/app.22877

Ryan, C. A., Billington, S. L., & Criddle, C. S. (2017). Methodology to assess end-of-life anaerobic biodegradation kinetics and methane production potential for composite materials. Composites Part A: Applied Science and Manufacturing, 95, 388–399. https://doi.org/10.1016/j.compositesa.2017.01.014

Srubar, W. V., & Billington, S. L. (2013). A micromechanical model for moisture-induced deterioration in fully biorenewable wood–plastic composites. Composites Part A: Applied Science and Manufacturing, 50, 81–92. https://doi.org/10.1016/j.compositesa.2013.02.001

Srubar, W. V., Michel, A. T., Criddle, C. S., Curtis Frank, W., & Billington, S. L. (2011). Engineered biomaterials for construction: a cradle-to-cradle design methodology for green material development. The International Journal of Environmental, Cultural, Economic and Social Sustainability, 7(5), 157e66.

Srubar, Wil V. (2015). An analytical model for predicting the freeze–thaw durability of wood–fiber composites. Composites Part B: Engineering, 69, 435–442. https://doi.org/10.1016/j.compositesb.2014.10.015

Srubar, Wil V., Frank, C. W., & Billington, S. L. (2012). Modeling the kinetics of water transport and hydroexpansion in a lignocellulose-reinforced bacterial copolyester. Polymer, 53(11), 2152–2161. https://doi.org/10.1016/j.polymer.2012.03.036

Väisänen, T., Haapala, A., Lappalainen, R., & Tomppo, L. (2016). Utilization of agricultural and forest industry waste and residues in natural fiber-polymer composites: A review. Waste Management, 54, 62–73.

Wang, W., & Morrell, J. J. (2004). Water sorption characteristics of two wood-plastic composites. Retrieved from http://ir.library.oregonstate.edu/xmlui/handle/1957/26271.